

Light Sheet Fluorescence Microscopy optimised for long-term imaging of Arabidopsis root development

Paolo Baesso, Ricardo S. Randall and Giovanni Sena*

* Corresponding author:

Giovanni Sena

Imperial College London,

Department of Life Sciences,

SW7 2AZ, London, UK

Running title: LSFM for Arabidopsis root

Abstract

Light Sheet Fluorescence Microscopy (LSFM) allows sustained and repeated optical sectioning of living specimens at high spatial and temporal resolution, with minimal photo-damage. Here, we describe in detail both the hardware and the software elements of a live imaging method based on LSFM and optimized for tracking and 3D-scanning of *Arabidopsis* root tips grown vertically in physiological conditions. The system is relatively inexpensive and with minimal footprint, hence it is well suited for laboratories of any size.

Keywords: Microscopy, Live imaging, Morphodynamics, *Arabidopsis* root, Tracking, Control software.

1 Introduction

Live imaging is a necessary tool to characterize the dynamics in developmental processes. While the details of the phenomenon under investigation will dictate the optimal magnification, spatial resolution, frequency of observations (temporal resolution) and duration of the observation, it is also crucial that the sample is kept alive, in the field of view and in focus during the entire session. Fluorescence microscopy offers many advantages, especially when internal tissues are to be imaged. If the sample is relatively transparent, a common solution is optical sectioning, usually achieved through one of the existing realizations of confocal microscopy [1]. Unfortunately, such methods rely on scanning the sample with a laser beam focused on a single point, resulting in high energy levels absorbed locally by the tissue. Therefore, frequent and prolonged time-lapse imaging through confocal microscopy can easily lead to severe damage and possibly death of the specimen [2]. Light-Sheet Fluorescence Microscopy (LSFM), or Selective Plane of Illumination Microscopy (SPIM), is an alternative to standard confocal microscopy that in the past few years has been successfully applied to developmental biology [3, 4]. A confocal microscope illuminates a large portion of the sample but collects emitted light only from a thin focal plane (thus effectively realising optical sections in the emission step). LSFM instead focuses the laser beam into a thin “sheet” of light to illuminate at once only a small portion of the sample at any given time (thus achieving actual optical sectioning), while collecting all light emitted in the direction perpendicular to the sheet [5]. LSFM results in significantly less energy being absorbed by the tissue, allowing prolonged and frequent observations [6].

The root of *Arabidopsis thaliana* is a popular model system for studying dynamic processes related to plant development and physiology. Its diameter is on average between 100 and 150 microns and it is almost completely optically transparent, making it an ideal tissue for fluorescence live imaging. Many key developmental and physiological processes (*e.g.* lateral root formation, tissue repair and regeneration, hormone and ion fluxes, etc.) exhibit rapid dynamics over relatively long periods. For the reasons described above, LSFM offers unique advantages for studying these processes at high spatial and temporal resolutions, by generating a long time-lapse series of frequent optical sections of growing *Arabidopsis* roots.

Since pioneering works originally demonstrated the successful application of LSM to Arabidopsis roots [7, 8], other setups have been developed to expand the potentials of the system [9]. To date, LSM has been used with Arabidopsis roots to study cell division dynamics [7, 10], lateral root formation [8, 11-14], calcium dynamics [15, 16], cell plate formation and root hair growth [17] and developmental zonation [18].

Full protocols have been published, developed around custom-made setups based on the design originally used in animal systems [19], a compact version inspired by the open-source hardware vision [20] and a commercial platform sold by Zeiss [21]. More recently, innovative hardware additions have been developed independently [10, 22].

Here, we provide a comprehensive description of the protocols for the development of both hardware and software for one of the simplest versions of LSM adapted for Arabidopsis roots. The setup is optimized for sustaining long-term (days) vertical growth of the primary root, whose tip is automatically tracked and scanned in 3D every few minutes. All the optical and motorized elements can be purchased off-the-shelf, a couple of custom-made parts can be easily 3D-printed, while the control software is written in MATLAB and freely available on a dedicated repository on GitHub.

2 Materials

2.1 Optics and motors

All the optical elements of the system are installed on a pneumatic optical table to reduce vibrations. Figure 1 shows a schematic of the setup.

1. Laser. The excitation beam is produced by a free space laser diode (Figure 1A). The laser wavelength is chosen based on the fluorophore excitation spectrum; the power requirement depends on the abundance and properties of the fluorophore, the sensitivity of the CCD camera and the quality of the optics: in our setup, a power between 10mW and 30mW is used.
2. Illumination optics group. The laser-beam passes through a series of optical elements to generate the thin “sheet of light” used for the excitation of the sample. Specifically: an interlock safety shutter (Figure 1B), a remotely controlled shutter (Figure 1C), a filter wheel (Figure 1D) carrying neutral density filters to adjust the laser power, a Galilean expander (Figure 1E) to increase the laser-beam diameter, an iris aperture (Figure 1F) to shape the beam diameter and a cylindrical lens (Figure 1G) (see **Note 1**).
3. Stage and sample chamber. The sample is located in a custom-made Growth and Imaging Cuvette (GIC, described below) (Figure 1H) positioned to locate the sample at the focal point of the cylindrical lens (see **Note 2**). The GIC is mounted on a 3-axis motorized stage that allows translating the sample in a 25.4 mm range with 0.05 μm precision in all three dimensions.
4. Imaging optics group. The light emitted by the sample is collected by a series of optical elements, mounted perpendicularly to the illumination axis, and focused on the CCD detector of a commercial microscope camera (Figure 1L). This is achieved by coupling an infinity-corrected objective (Figure 1I) with a tube lens (Figure 1K). A motorized filter wheel carries band-pass filters (Figure 1J) that can be inserted between objective and tube lenses. The band pass range must be selected so that it encompasses the excitation wavelength. A manual turret can be used to change magnification by switching between different objectives. The distance between the objective and the GIC can be adjusted using a secondary motorized stage located under the imaging optics.

5. Enclosure. To maintain the system in darkness and obtain optimal imaging conditions, the illumination and imaging groups, together with the stage and the GIC, are enclosed in a box equipped with movable windows to access the system. A custom-made LED cluster is mounted on the roof of the box, above the sample holder, to illuminate the seedling between imaging events.

2.2 Growth and Imaging Cuvette (GIC)

All of the below, other than the plastic cuvette, must be autoclaved prior to use (see **Note 3**).

Figure 2 shows the main parts of the GIC and the steps used to mount the specimen in it.

1. 3.5 mL optical quartz cuvette with internal dimensions of 10 mm x 10 mm x 40 mm.
2. 0.5 mm diameter stainless steel pin, cut to match the internal height of the cuvette.
3. A soft sleeve to be used around the pin, which will be pushed into the corner of the cuvette to create the channel for the root (see **Note 4**). Crucially, the sleeve is shorter than the pin, so that the liquid medium can diffuse in and out of the channel from the top and the bottom of it.
4. 1 mm and 2 mm diameter glass beads.
5. 3D-printed nylon joint (Figure 3), to connect the GIC to the perfusion system (see **Note 5**). The joint has an inlet path bringing fresh medium to the cuvette, and an outlet path removing spent medium from the top of the cuvette.
6. Dispensing needle, to be connected to the nylon joint to inject the fresh medium at the bottom of the cuvette.
7. Plastic “top” cuvette, with cut-out windows covered by breathable tape on the side, and closed at the top with a glass coverslip.
8. The GIC is positioned in the ad-hoc, 3D-printed, holder sitting on the motorized stage, as shown in Figure 1H and Figure 5.

2.3 Perfusion system

Nutrients and oxygen are provided to the plant by means of a continuous perfusion system. Its main components are shown in Figure 4 (see **Note 6**).

1. Air pump (Figure 4A) connected to a porous “air” stone, to oxygenate the medium in the reservoir bottle (Figure 4C).
2. Air filters (Figure 4B, E).
3. Reservoir bottle (Figure 4C), containing sterile medium (see **Note 7**).
4. Cold trap (Figure 4D), to condensate and capture water vapour in the vented air escaping the reservoir (see **Note 8**).
5. Peristaltic pump (Figure 4F), to drive the feeding line.
6. Peltier cell (Figure 4G), to control the temperature of the feeding line.
7. GIC (Figure 4H), as described above.
8. Waste bottle (Figure 4I), to collect the spent medium from the waste line.
9. Vacuum pump (Figure 4J), to drive the waste line.
10. Inflow (blue) and outflow (red) silicone tubing.

2.4 Temperature and light control systems

The temperature of the medium in the inflow line is continuously monitored and automatically adjusted with a Peltier cell via feedback control. The seedling is illuminated by an LED cluster only between imaging scans.

1. Infrared sensor, controlled via an Arduino board and mounted in front of the GIC (Figure 5) to remotely monitor the temperature of the liquid medium.
2. Heat exchanger element (Figure 6), constituted by a Peltier cell held in contact with a serpentine by a 3D-printed clamp. The Peltier cell is controlled through a separate Arduino board controlled via MATLAB.
3. A single cluster of 40 LEDs is installed approximately 10 cm above the cuvette. The cluster has been designed to provide uniform illumination at wavelengths 465 nm, 635 nm and 650 nm (Figure 7). The cluster switch is controlled through a LabJack board using MATLAB.

2.5 Control software

The following system components are under the control of a single program developed in MATLAB: laser shutters, GIC stage motors (x, y, z axes), emission filter wheel, camera stage motors (x, y axes), LED cluster, perfusion inflow peristaltic pump, Peltier cell, infrared temperature sensor. A Graphical User Interface (GUI) allows the operator to control the system and to run an automated imaging routine. The automated routine is composed by a sequence of steps repeated at a fixed interval of time. See Methods for a detailed description of each step.

The MATLAB software to control the system and provide the GUI is stored in a dedicated GitHub repository: <https://github.com/GiovanniSena/LSFM>

2.6 Plant material and solutions

1. As presented, the protocol is designed to be used with *Arabidopsis thaliana*, but not limited to any specific genetic background. Since the system is based on fluorescence microscopy, a fluorescent reporter or dye must be present.
2. Sterilization solution: 50% v/v house bleach, 0.05% v/v Triton X-100.
3. Solid medium (agar plates): 1X Murashige and Skoog (MS) Basal Medium, 0.5% w/v sucrose, 0.05% w/v MES hydrate, 0.8% w/v agar, pH 5.7 with KOH.
4. Liquid medium (perfusion): ¼X Murashige and Skoog (MS) Basal Medium with Gamborg's vitamins, 0.5% w/v sucrose, 0.05% w/v MES hydrate, pH 5.7 with KOH.

3 Methods

3.1 Agar plates for seed germination

1. Fill a 1L beaker containing a magnetic stir bar with 900mL water and add 5g sucrose, 0.5g MES hydrate and 1.75g MS. Use a magnetic stirring plate to dissolve the reagents. Once dissolved, add

KOH until the solution reaches pH 5.7, then make the solution up to 1L with distilled water. Add 8g agar.

2. Autoclave. The media may be kept for several hours in an oven with a temperature of 55°C.
3. Pour the medium into sterile petri dishes under sterile conditions.

3.2 Seed sterilisation and germination

Perform the following under sterile conditions:

1. Resuspend seeds in sterilization solution for 3 minutes. Immediately rinse the seeds with sterile water. Repeat the rinsing six more times to eliminate bleach residues.
2. To synchronize seed germination, stratification is applied by keeping the sterile seeds in the dark and at 4°C for 2 days before transferring onto a solid agar plate.
3. Using a sterile plastic transfer pipette (see **Note 9**) place the seeds onto an MS agar plate. The seedlings will need up to 3 cm of space underneath the seed for growth of the root. Seal each plate with either Parafilm or breathable tape, to minimize the risk of contamination.
4. Place the plates in standard germinating conditions: 23°C with 120 $\mu\text{mol m}^{-2}\text{s}^{-1}$ light using a light/dark cycle of 16/8 hours (see **Notes 10, 11**).

3.3 Mounting the seedlings into the GIC

Perform the following under sterile conditions:

1. The seedlings should be mounted when the root is between 15 mm and 25 mm long, typically 3 or 4 days postgermination.
2. Before mounting, confirm the signal intensity from the root under a fluorescence stereo microscope.
3. Find the “optical surface” of the cuvette, as defined by the manufacturer, to identify the corner where the root will be located.
4. Use a small amount of MS liquid medium to wet the corner of the cuvette. The surface tension of the liquid facilitates the correct positioning of the root.
5. Remove the seedling from the plate using sterile forceps and carefully position the root in the wet corner (see **Note 12**) (Figure 2A). Ideally, the entire length of the root should be in the cuvette, while the hypocotyl and cotyledons should protrude from its top. The correct position of the root should be checked after each of the following steps.
6. Using sterile forceps, gently position the pin in the cuvette, to trap the root in the corner (see **Note 13**) (Figure 2B, G).
7. Slowly fill the cuvette with some of the perfusion medium and the 2 mm glass beads (see **Note 14**) (Figure 2C).
8. Fill the rest of the cuvette with 1 mm glass beads, up to about 10 mm from the top of the cuvette (Figure 2D).
9. Attach the nylon joint to the dispensing needle via the Luer lock, and gently push the needle through the beads, until the joint sits tightly in the cuvette, effectively capping it (Figure 2E).
10. Slide the plastic “top” cuvette over the insert, taking care not to pinch the cotyledons. Seal the cuvettes together using breathable tape (Figure 2F).

3.4 Starting the perfusion

Use Figure 4 as reference for the parts mentioned here.

1. At the beginning of the experiment, the reservoir bottle is filled with sterile liquid medium.
2. Mount the feeding line into the peristaltic pump (see **Note 15**).
3. Under sterile conditions, insert the air stone connected to the air line in the reservoir bottle; ensure that this bottle contains a magnetic stir bar. Do not yet turn on either the air pump or the peristaltic pump.
4. Start stirring the medium on the stirring plate.
5. Connect the feeding line to the serpentine connected to the Peltier cell.
6. Connect the other end of the serpentine to the waste line, thus bypassing the GIC and closing the circuit.
7. Connect the waste bottle to the vacuum pump.
8. Turn on the air pump (to bubble air into the reservoir), the peristaltic pump (to circulate the feeding line) and the vacuum pump (to start the suction in the waste line), in this order.
9. Let the system prime until the feeding line is completely filled with medium (see **Note 16**), then stop the air, peristaltic and vacuum pumps, in this order.
10. Prime the short tubing connected to the GIC's feeding inlet, using a manual syringe to inject liquid medium until it reaches the hypocotyl of the seedling in the GIC.
11. Position and secure the GIC on the microscope's holder (Figure 1H).
12. Slightly loosen the cap of the waste bottle, to eliminate any residual negative pressure from the waste line.
13. Disconnect the waste line from the serpentine, and connect it to the outflow inlet of the GIC.
14. Connect the serpentine to the inflow inlet of the GIC. The circuit should now be closed again, with the GIC between the serpentine and the waste bottle (Figure 4).
15. Tighten the cap of the waste bottle.
16. Turn on, in this order: the vacuum pump, the air pump and finally the peristaltic pump (see **Note 17**).

3.5 Setting up initial conditions and starting the automated imaging

With the seedling mounted in the GIC (section 3.3) and the perfusion system operative (section 3.4), it is time to position the root in the field of view and to start the scanning.

1. Switch to brightfield conditions, by turning on the LEDs, closing the shutter and removing the emission filter.
2. Use the motors controlling the camera's position to find the root tip and to focus onto it (see **Note 18**).
3. Switch to fluorescence conditions by turning off the LEDs, opening the shutter and positioning the required emission filter.
4. The root is already in focus with the objective (point 2 above), but it will only fluoresce when it is illuminated by the light sheet: use the dedicated command on the software GUI to lock together the camera and the stage movements in the dimension perpendicular to the light sheet (to keep the root in focus), and move them until fluorescence emission from the root becomes visible (see **Note 19**).

5. Once fluorescence is observed, one should ensure that the root is illuminated by the thinnest part of the sheet (TPS), which is located at the focal point of the cylindrical lens. First, make sure that the camera and the stage movements are locked together in both dimensions (to keep the root in the field of view and in focus). Then apply small adjustments perpendicular to the light path, until the signal in emission reaches maximum intensity. Finally, apply small translations in the direction parallel to the light sheet and repeat the previous step. Since light is most concentrated at the TPS but it illuminates a smaller volume of the root, one can look for increased emission of the details in focus and decreased emission of those out of focus, as a proxy for being in the TPS.
6. Manually scan the root in the axial dimension (the direction perpendicular to the light sheet, used to generate the stack of optical sections during automated acquisition) to determine (a) thickness of the root in microns, (b) position of the root's surface closest to the objective.
7. Unlock stage and camera movements.
8. Manually focus on the root's surface closest to the objective.
9. Use the parameters in the *Config* panel of the GUI to specify: (a) scanning step length (usually 4 μ m), (b) total number of steps (root's diameter measured in step 6, plus some buffer space on either side of the root), (c) temporal interval between scans (usually 10 minutes), (d) temperature to maintain in the GIC liquid medium (usually 23 °C) (see **Note 20**).
10. In the GUI, start the automated scan.

3.6 Automated z-stack acquisition

1. At each programmed time-point a 3D stack of optical sections is created by moving the root through the light sheet in steps and recording an image at each position.
2. During the scan, a standard autofocus routine [23] is executed at intervals defined by the user.
3. The raw data of each stack is saved to disk and its Maximum Intensity Projection is visualized in the software GUI.
4. A new stack is acquired at temporal intervals defined in the *Config* panel of the software (see point 9 in section 3.5)

3.7 Root tracking

A tracking algorithm was developed to determine the movement of the root tip between two subsequent scans and to adjust the cuvette position to maintain the root tip in the field of view. A root scan creates a stack of N grayscale images, which can be saved as a 3D matrix where each element is the intensity value of the pixel. In order to minimize the number of scans imposed on a root, and therefore to minimize any photo-damage, the tracking is solely based on the 3D stacks already acquired on the current and previous time points. In essence, it is assumed that in the previous time-point the root tip was in the centre of the field of view, and that in a single time interval it grew only slightly out of it.

The actual steps involved are (Figure 8):

1. Acquire 3D stack at time t : image I_t . If this is the first image of the scan, the system pauses until the required time has elapsed. Similarly, if the user has manually adjusted the motors, the system treat the stack as if it were the first of a new acquisition.
2. Retrieve the virtually transformed stack obtained at time $t-1$ (see below): image \tilde{I}_{t-1} .

3. Rescale I_t and \tilde{I}_{t-1} , to reduce the computational time required for the tracking algorithm. The scaling factor is defined by the user and is typically equal to 2 in X and Y (*i.e.* the image size is reduced by a factor 4).
4. Extract a region of interest from the full stack, to further reduce computational time and to eliminate potential external objects (dead cells, optical artefacts, etc.), by removing a fixed $\{\Delta X, \Delta Y, \Delta Z\}$ region on the perimeter of the stack. For simplicity, the rescaled and cropped stacks are still referred to as I_t and \tilde{I}_{t-1} .
5. Registration is performed to find the new transformation matrix A_{tr} (see **Note 21**), such that

$$I_t = A_{tr} \cdot \tilde{I}_{t-1}$$

The algorithm used to determine A_{tr} is based on the mean square error of the pixel intensities and uses a standard iterative step gradient descent to estimate the best transformation [24] (see **Note 22**).

6. Stage movement: the stages holding the GIC are moved “back” accordingly to A_{tr}^{-1} , to bring the root tip back in the center of the field of view.
7. Virtual movement: instead of taking a second scan of the now translated root (see above), the last image I_t is virtually (computationally) translated with A_{tr} to generate \tilde{I}_t , which will be uploaded as \tilde{I}_{t-1} at the beginning of the next time-point.
8. After the waiting time determined by the user is elapsed, the routine is repeated from step 1.

3.8 Temperature control

While the GUI is running, the temperature of the cuvette is monitored through the IR sensor (Fig 5A). If the temperature drops below a user-defined threshold (T_{target}), the software activates the Peltier cell and provides energy to the heat exchanger. The energy provided to the cell is increased linearly as a function of the difference between the current temperature T and T_{target} .

In our setup, the Peltier cell was configured to act as a heater but an identical cell could easily be installed to provide cooling capabilities as well.

3.9 Cleaning and maintenance

1. Stop the pumps.
2. Uncouple the GIC from the perfusion system and remove it from the stage.
3. Close the perfusion circuit by connecting together the feeding and the waste lines.
4. Remove the air stone and the feeding tube from the media bottle and place them in a new bottle containing hot clean water, pumping air through the stone and circulating the hot water through the closed system for at least 45 minutes.
5. Clean the cuvette using optical glass cleaning solution and lens wipes; rinse it with 100% isopropanol and air dry it.
6. Use a syringe to flush the tubes attached to the cuvette, and the feeding needle still mounted on the insert, with hot water.
7. Wrap all items in individual autoclave bags and autoclave.

4 Notes

1. The shape of the illumination beam after the cylindrical lens is determined by two factors: the minimum width w_0 of the sheet of light (or Thinnest Part of the Sheet, TPS, at the focal point of the cylindrical lens) and its extension, Δx (or for how long the sheet's minimum thickness is maintained in the dimension parallel to the laser beam).

These parameters are approximated by:

$$w_0 \cong 1.22 \lambda \frac{f}{d}$$
$$\Delta x \cong \frac{2\pi}{\lambda} w_0^2$$

Where λ is the laser wavelength, f is the focal length of the cylindrical lens and d is the beam diameter hitting the cylindrical lens (*i.e.*, the iris aperture). The laser wavelength will have to be determined on the basis of the fluorophore to be imaged. We currently use genetic reporters tagged with GFP or YFP, and we chose a laser with $\lambda = 488 \text{ nm}$; we chose to use a lens with $f = 50 \text{ mm}$ and $d = 7.5 \text{ mm}$ to obtain nominal values $w_0 \cong 4 \mu\text{m}$ and $\Delta x \cong 203 \mu\text{m}$, which are compatible with a desirable axial resolution (*e.g.* the average distance between cell nuclei is $> 4 \mu\text{m}$) and a typical Arabidopsis root diameter. Notice that the optical expander must be chosen so that the diameter of the expanded beam is sufficient to cover the whole iris aperture. After the cylindrical lens, the laser beam travels through air, glass (cuvette wall), and aqueous medium before reaching the sample in the cuvette. The optical path is therefore composed by multiple indexes of refraction, and the exact position of the cylindrical lens focal point (the actual location of the TPS) will have to be determined empirically. We use fluorescent beads embedded in Phytigel to visualize the light sheet profile and precisely determine the position of the TPS inside the cuvette.

2. Maintaining the root in the objective's field of view and in focus while it is growing requires subsequent adjustments of the camera position. Our custom control software contains specific automated "tracking" and "focusing" routines designed to automatically move the camera and follow the root movements (see the software description). For this reason, the objective and the camera are rigidly connected and mounted on a second motorized stage able to translate in x and y.
3. It is important that all items that come into contact with the specimen and growth media are sterile and free of compounds that might be toxic to the seedling. Most components can be autoclaved, with the exception of the plastic cuvette and microporous tape. To reduce the likelihood of potentially toxic compounds accumulating on the surfaces of items during autoclaving, we use small autoclaving bags, commonly used for the sterilization of surgical tools.
4. We find that electrical heat-shrink tubing works well as a soft sleeve around the pin. Fit a length of this sleeve over the pin that leaves 3 mm of needle exposed at either end; use a source of heat, such as a heat gun, to shrink the sleeve onto the pin. The actual size of the channel in the cuvette's corner is determined by the total diameter of the pin + sleeve element pushed against the cuvette corner. Elementary geometry indicates that $d \cong 0.17 D$, where d is the maximum diameter of a cylinder (*i.e.* the root) fitting in the channel, and D is the diameter of the combined pin + sleeve element. We currently use a pin with diameter $500 \mu\text{m}$ and a sleeve with thickness $450 \mu\text{m}$, resulting in $d = 240 \mu\text{m}$.
5. The insert should be 3D-printed in nylon or any other material capable of withstanding the autoclaving process.

6. We use autoclavable silicone tubing connected by means of quick-release shut-off couplings. This facilitates the set-up of the perfusion system and allows us to quickly replace the reservoir and waste bottles during prolonged experiments, while maintaining sterile conditions.
7. The medium in the reservoir bottle should be maintained well mixed during the experiment. For this purpose, we keep a magnetic bar in it and place the bottle on a large stirring plate.
8. The relief line is needed to maintain the pressure within the bottle at equilibrium with the atmospheric pressure. The excess of air introduced by the air pump escapes through this route via a filter to reduce the risk of contamination of the medium. The cold trap reduces the risk of condensation within the filter, which would cause its occlusion.
9. We keep the sterile seeds resuspended in sterile water, and use a plastic transfer pipette to dispense one seed at a time on the solid agar plate. Since the seedlings will not be grown for long on the plate, little space is needed between seeds i.e. 5 mm horizontally and ca. 30 mm vertically.
10. To minimize the possibility of the cotyledons being submersed at any time during the experiment, a mild etiolation increase the distance between the cotyledons and the root can be considered. To ensure proper growth of the cotyledons prior to mounting in the GIC, two days of normal growth should follow etiolation. Thus, one would grow the seedlings in the dark for two days following germination and a subsequent two days in standard light/dark cycle conditions.
11. The transition between the “germinating” light/dark regime and the “imaging” one might result in physiological stress to the plant. Depending on the scope of the experiment, it might be considered to germinate the seeds already under the “imaging” regime, simulating the same alternation of light and darkness that the seedlings will then experience in the GIC.
12. To ensure that the seedling does not dry out during the mounting procedure, one can use a nebuliser loaded with sterile water, to increase the relative humidity of the air in the working area.
13. It is crucial that the pin traps the root in the corner of the cuvette. To achieve this, position one end of the pin in the cuvette’s bottom corner and carefully pivot around it to ensure that the pin is positioned as in Figure 2C. Using a magnifying lens, make sure that the root is indeed located within the channel formed between pin and cuvette walls. If not, repeat this step.
14. The beads will push on the pin and hold it in position.
15. It is critical that the feeding line is properly and fully mounted in the peristaltic pump. It might be easier to perform this step when the line is still empty of fluid.
16. This is critical to eliminate air bubbles from the feeding line. They would disturb the root during acquisition.
17. To avoid flooding, before turning on the peristaltic pump regulating the inflow, make sure that the vacuum pump is creating enough negative pressure in the waste bottle, and that suction in the GIC is working adequately.
18. This is best achieved with a low magnification objective, such as 10x or 20x.
19. Once some signal is detected by the camera (*i.e.* the root is now illuminated by the light sheet), focusing might be required. Unlock the camera movement from the stage, and apply small steps on the camera to bring the root back in focus. Then lock the movements again.
20. The temporal interval between scans defines the temporal resolution of the dataset. A few considerations must be taken into account when choosing this parameter, to find the right balance between conflicting priorities: root tracking works better with small temporal intervals; during scanning the LEDs are off, therefore scanning too frequently limits the photosynthetic yield of the seedling; frequent imaging may also result in photo-toxicity for the plant or photo-bleaching for the fluorophore.

21. Since the stage can only be translated linearly, we impose A_{tr} to represent a simple rigid translation in 3D, which will effectively represent the more complex roto-translation of the root tip. The MATLAB function used for this is *imregtform*.
22. Note that this tracking routine does not depend on the conical shape of the root tip, so it is equally amenable for uncut as well as regenerating tissue.

5 References

1. Yuste R (2011) *Imaging: a laboratory manual*. CSH Press, New York
2. Dixit R, Cyr R (2003) Cell damage and reactive oxygen species production induced by fluorescence microscopy: effect on mitosis and guidelines for non-invasive fluorescence microscopy. *The Plant Journal* 36:280–290. doi: 10.1046/j.1365-313X.2003.01868.x
3. Huisken J, Swoger J, Del Bene F, et al (2004) Optical sectioning deep inside live embryos by selective plane illumination microscopy. *Science* 305:1007–1009. doi: 10.1126/science.1100035
4. Huisken J, Stainier D YR (2009) Selective plane illumination microscopy techniques in developmental biology. *Development* 136:1963–1975. doi: 10.1242/dev.022426
5. Greger K, Swoger J, Stelzer EHK (2007) Basic building units and properties of a fluorescence single plane illumination microscope. *Rev Sci Instrum* 78:023705.
6. Reynaud EG, Krzic U, Greger K, Stelzer EHK (2008) Light sheet-based fluorescence microscopy: more dimensions, more photons, and less photodamage. *HFSP J* 2:266–275. doi: 10.2976/1.2974980
7. Sena G, Frentz Z, Birnbaum KD, Leibler S (2011) Quantitation of cellular dynamics in growing *Arabidopsis* roots with light sheet microscopy. *PLoS One* 6:e21303. doi: 10.1371/journal.pone.0021303
8. Maizel A, Wangenheim von D, Federici F, et al (2011) High-resolution live imaging of plant growth in near physiological bright conditions using light sheet fluorescence microscopy. *Plant J* 68:377–385. doi: 10.1111/j.1365-313X.2011.04692.x
9. Berthet B, Maizel A (2016) Light sheet microscopy and live imaging of plants. *J Microsc* 263:158–164. doi: 10.1111/jmi.12393
10. de Luis Balaguer MA, Ramos-Pezzotti M, Rahhal MB, et al (2016) Multi-sample *Arabidopsis* Growth and Imaging Chamber (MAGIC) for long term imaging in the ZEISS Lightsheet Z.1. *Dev Biol* 419:19–25. doi: 10.1016/j.ydbio.2016.05.029
11. Lucas M, Kenobi K, Wangenheim von D, et al (2013) Lateral root morphogenesis is dependent on the mechanical properties of the overlaying tissues. *Proceedings of the National Academy of Sciences* 110:5229–5234. doi: 10.1073/pnas.1210807110
12. Rosquete MR, Wangenheim von D, Marhavý P, et al (2013) An Auxin Transport Mechanism Restricts Positive Orthogravitropism in Lateral Roots. *Curr Biol* 23:817–822. doi:

- 10.1016/j.cub.2013.03.064
13. Vermeer JEM, Wangenheim von D, Barberon M, et al (2014) A Spatial Accommodation by Neighboring Cells Is Required for Organ Initiation in Arabidopsis. *Science* 343:178–183. doi: 10.1126/science.1245871
 14. Wangenheim von D, Fangerau J, Schmitz A, et al (2016) Rules and Self-Organizing Properties of Post-embryonic Plant Organ Cell Division Patterns. *Curr Biol* 26:439–449. doi: 10.1016/j.cub.2015.12.047
 15. Costa A, Candeo A, Fieramonti L, et al (2013) Calcium Dynamics in Root Cells of Arabidopsis thaliana Visualized with Selective Plane Illumination Microscopy. *PLoS One* 8:e75646. doi: 10.1371/journal.pone.0075646.s012
 16. Candeo A, Doccula FG, Valentini G, et al (2017) Light Sheet Fluorescence Microscopy Quantifies Calcium Oscillations in Root Hairs of Arabidopsis thaliana. *Plant Cell Physiol*. doi: 10.1093/pcp/pcx045
 17. Berson T, Wangenheim von D, Takáč T, et al (2014) Trans-Golgi network localized small GTPase RabA1d is involved in cell plate formation and oscillatory root hair growth. *BMC Plant Biology* 14:252. doi: 10.1186/s12870-014-0252-0
 18. Novák D, Kuchařová A, Ovečka M, et al (2015) Developmental Nuclear Localization and Quantification of GFP-Tagged EB1c in Arabidopsis Root Using Light-Sheet Microscopy. *Front Plant Sci* 6:1187. doi: 10.3389/fpls.2015.01187
 19. Wangenheim von D, Daum G, Lohmann JU, et al (2014) Live imaging of Arabidopsis development. *Methods Mol Biol* 1062:539–550. doi: 10.1007/978-1-62703-580-4_28
 20. Wangenheim von D, Hauschild R, Friml J (2017) Light Sheet Fluorescence Microscopy of Plant Roots Growing on the Surface of a Gel. *J Vis Exp*. doi: 10.3791/55044
 21. Ovečka M, Vaškebová L, Komis G, et al (2015) Preparation of plants for developmental and cellular imaging by light-sheet microscopy. *Nature Protocols* 10:1234–1247. doi: 10.1038/nprot.2015.081
 22. Jeandupeux E, Lobjois V, Ducommun B (2015) 3D print customized sample holders for live light sheet microscopy. *Biochem Biophys Res Commun* 463:1141–1143. doi: 10.1016/j.bbrc.2015.06.072
 23. Geusebroek JM, Cornelissen F, Smeulders A, Geerts H (2000) Robust autofocusing in microscopy. *Cytometry* 39:1–9.
 24. van der Bom IMJ, Klein S, Staring M, et al (2011) Evaluation of optimization methods for intensity-based 2D-3D registration in x-ray guided interventions. In: Dawant BM, Haynor DR (eds) 2011 8th IEEE International Symposium on Biomedical Imaging (ISBI 2011). International Society for Optics and Photonics, pp 796223–796223–15

Acknowledgments

This work was supported by BBSRC grant BB/M002624/1.

Figure Captions

Figure 1: Schematic of the main optical components of the light sheet microscope setup. The elements are mounted on a pneumatic optical table (not shown in the figure) and controlled remotely via MATLAB software. A, laser module; B, safety shutter; C, shutter; D, neutral density filter wheel; E, beam expander; F, iris; G, cylindrical lens; H, sample chamber (GIC); I, objective; J, emission filter wheel; K, tube lens; L, CCD camera.

Figure 2: Mounting the seedling within the GIC. A, the seedling is positioned in the glass cuvette, with the root laying in one of the corners (arrow); B, the pin with its black sleeve (arrow) constrains the root in the corner; C, large beads ($\varnothing = 2$ mm) on the bottom of the cuvette, to hold the pin in position (arrow); D, small beads ($\varnothing = 1$ mm) filling the rest of the cuvette; E, the nylon joint inserted in the cuvette; F, the complete GIC, connected to the perfusion tubings and sealed with micropore tape (arrow); G, schematic of the assembled GIC (beads not shown); H, schematic of GIC with the beads. Details: u, glass cuvette; v, pin with sleeve; w, dispensing needle; x, nylon joint; y, top cuvette; z, root in the corner of the cuvette. Bar, 10 mm.

Figure 3: Drawings of the nylon joint. Measurements in mm.

Figure 4: Schematic of the perfusion system with its main components. The feeding line is shown in blue, the waste line in red. Air lines are shown in black. Arrows indicate the direction of flow. A, air pump; B, air filter; C, media bottle; D, cold trap; E, air filter; F, peristaltic pump; G, Peltier cell; H, GIC; I, waste media bottle; J, vacuum pump.

Figure 5: Schematic close-up of the cuvette holder. A, IR temperature sensor; B, GIC; C, objective; D, cylindrical lens.

Figure 6: Schematic of the heat exchanger element used in the perfusion system.

Figure 7: Schematic of the different wavelengths used and their distribution in the LED cluster.

Figure 8: Block diagram of the main operations performed by the software during automated data acquisition.

Fig. 1

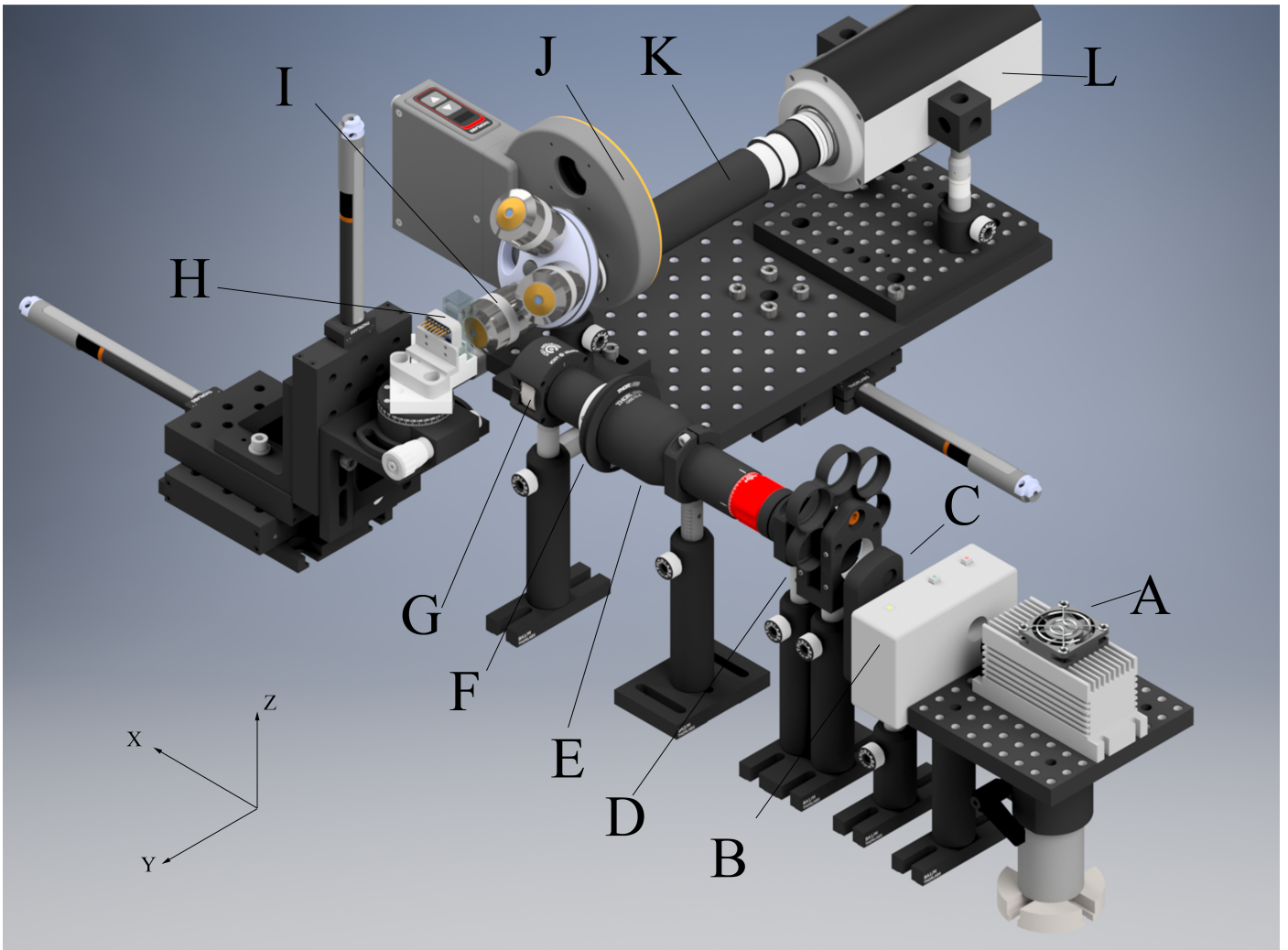


Fig. 2

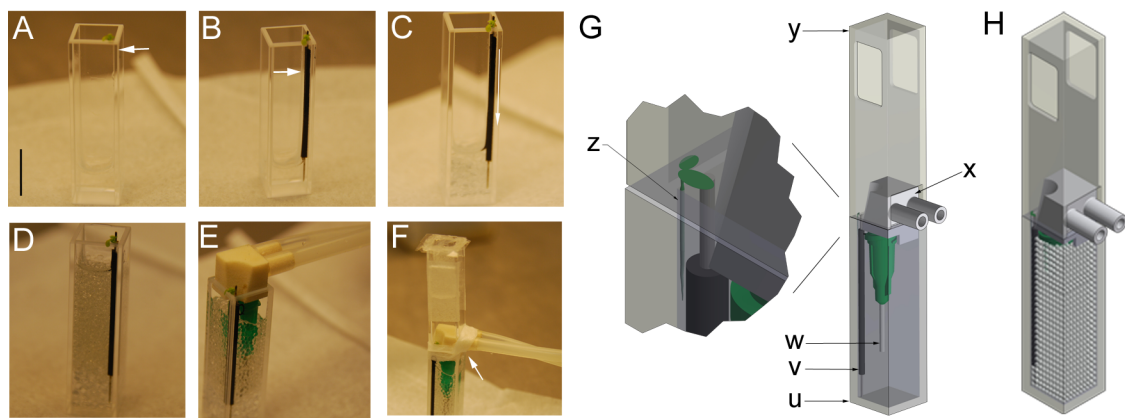


Fig. 3

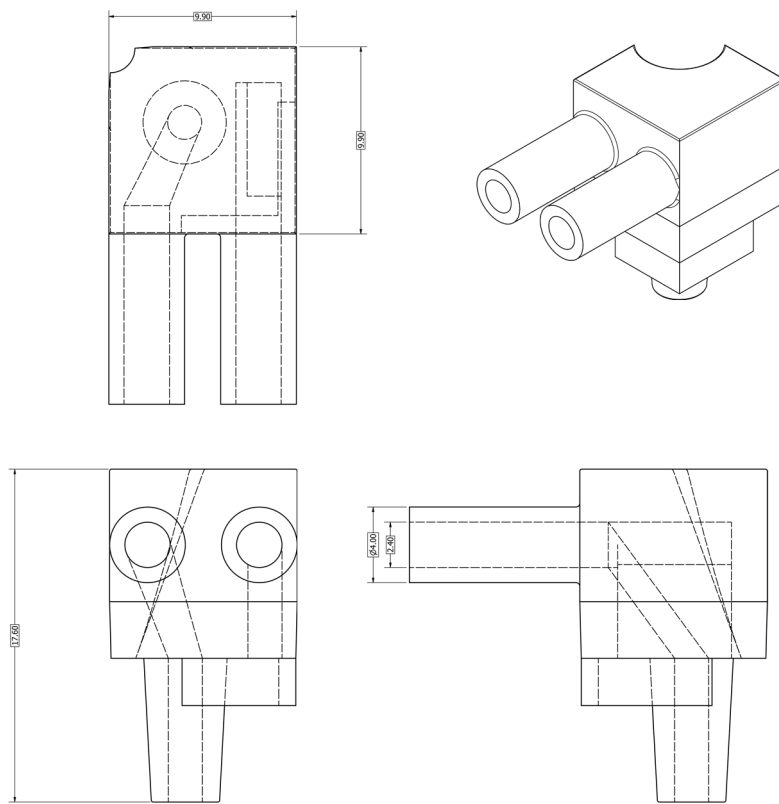


Fig. 4

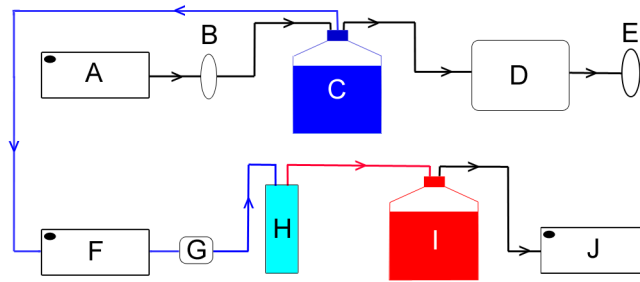


Fig. 5

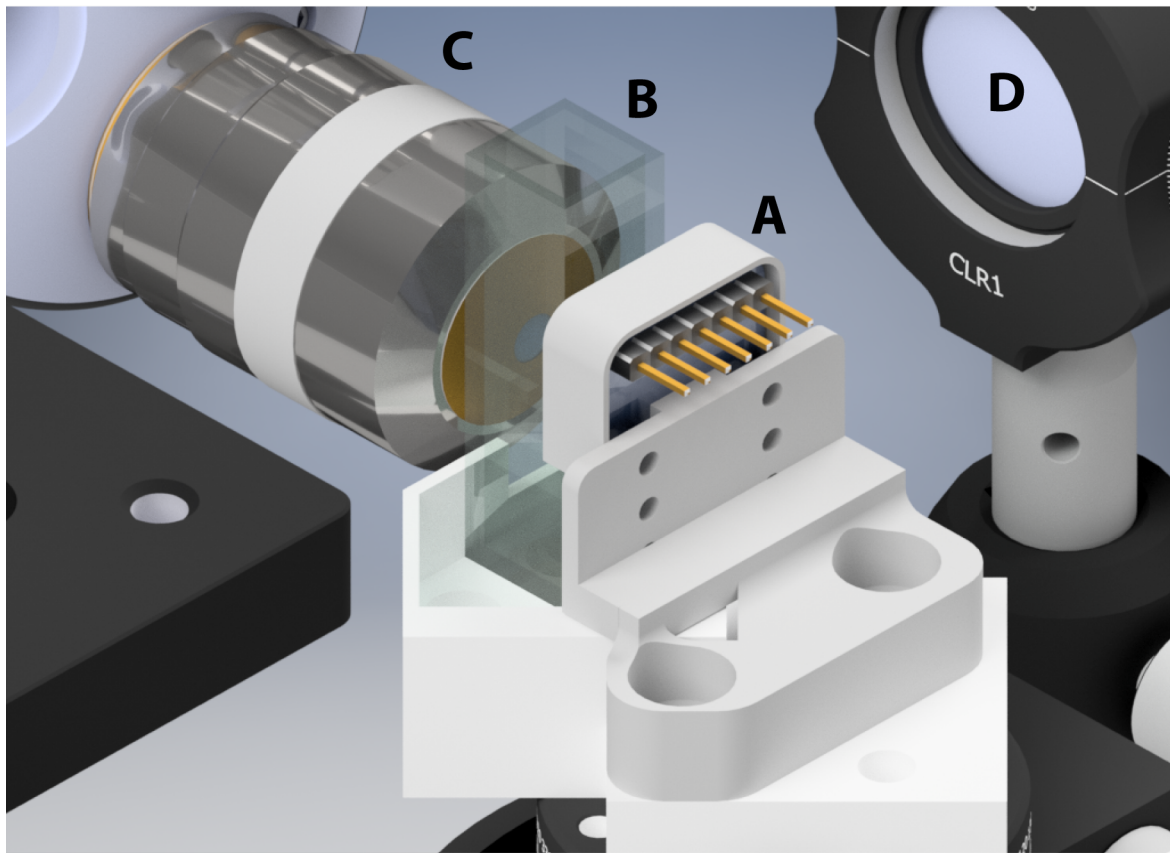


Fig. 6

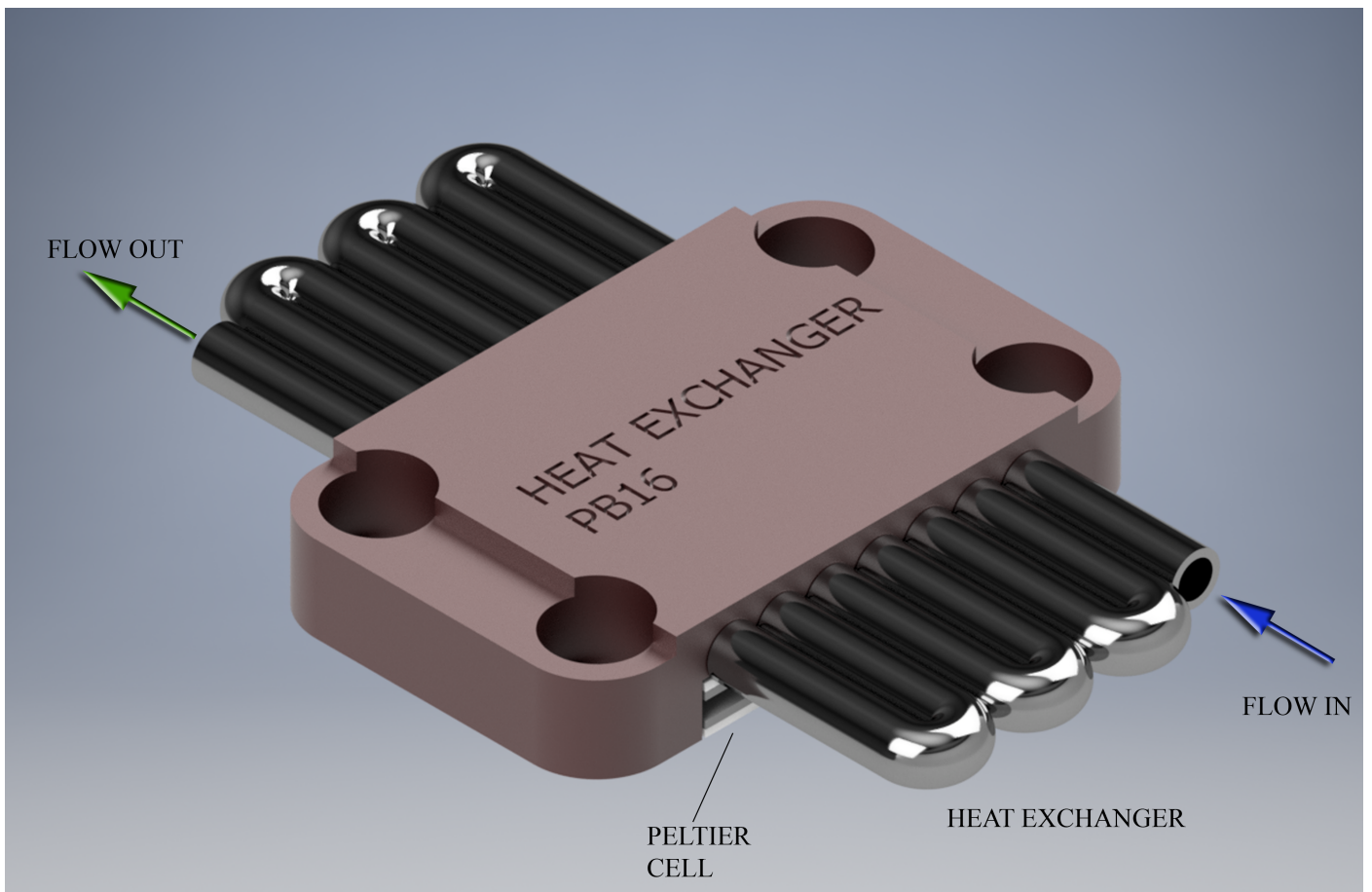


Fig. 7

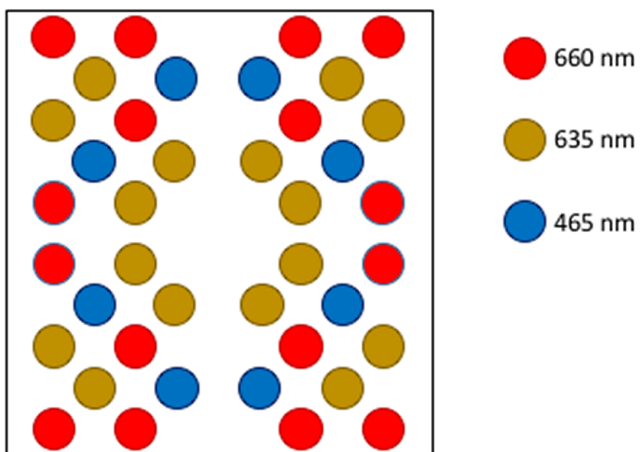


Fig. 8

